IL NUOVO CIMENTO **41 C** (2018) 141
DOI 10.1393/ncc/i2018-18141-5

COLLOQUIA: LaThuile 2018

Measurement of ϕ_s

M. LUCIO on behalf of the LHCb COLLABORATION

Universidade de Santiago de Compostela - Santiago de Compostela, Spain

received 6 September 2018

Summary. — Precision measurements are needed in order to properly disentangle Standard Model (SM) contributions from possible New Physics (NP) effects, that could greatly affect *CP* observables. This document reviews the latest results from LHCb concerning *CP* violation using Run-1 data, for the decays $B_s^0 \to J/\psi K^+K^-$, $B_s^0 \to (K^+\pi^-)(K^-\pi^+)$ and $B_s^0 \to \phi\phi$. The measurements presented for the first two channels are the world's best results obtained up to date. All the discussed results constitute a considerable improvement with respect to previous ones. The corresponding uncertainties on the measurements are expected to the decrease with updates using Run-2 data.

1. – Introduction

The Standard Model (SM) of particle physics fails to explain many experimental observations, such as the amount of matter-antimatter asymmetry observed in the Universe. The existence of new phenomena beyond those predicted by the SM, hereafter referred to as New Physics (NP), could introduce sizeable effects in *CP*-violating observables, thus explaining the aforementioned asymmetry. In the SM, *CP* violation originates from a single phase in the Cabibbo-Kobayashi-Maskawa (CKM) quark-mixing matrix [1]. There are 3 different kinds of *CP* violation for neutral mesons, *e.g.*, B_s^0 and $\bar{B}_s^0$:

1) Direct *CP* violation: originated by a difference in the amplitudes associated to the direct decay of the B_s^0 and $\bar{B}_s^0$ mesons into the same final state

2) *CP* violation in the B_s^0-$\bar{B}_s^0$ oscillation, that arises when the oscillation from B_s^0 to $\bar{B}_s^0$ is different from the oscillation from $\bar{B}_s^0$ to B_s^0

3) *CP* violation in the interference between the amplitudes associated to the direct decay of a B_s^0 meson into a *CP*-eigenstate final state and those associated to the decay after B_s^0-$\bar{B}_s^0$ oscillation

This last type of *CP* violation is characterized by the *CP*-violating phase, ϕ_s, defined as

$$\phi_s^f = -\arg(\lambda_f), \quad \lambda_f = \eta_f \frac{q}{p} \frac{\bar{\mathcal{A}}_f}{\mathcal{A}_f}, \tag{1}$$

where f is the final state, η_f is 1 (-1) for *CP*-even (*CP*-odd) states, $|\frac{q}{p}|$ determines the amount of *CP* violation in mixing, and $\mathcal{A}_f$ ($\bar{\mathcal{A}}_f$) is the amplitude of the B_s^0 ($\bar{B}_s^0$) meson decaying into a given final state, f.

Precision measurements of this phase are needed in order to properly disentagle SM and NP contributions. In this document, the latest results from the LHCb Collaboration on ϕ_s^f are reviewed in the $B_s^0 \to J/\psi K^+K^-$, $B_s^0 \to (K^+\pi^-)(K^-\pi^+)$ and $B_s^0 \to \phi\phi$ channels. All of them are performed using Run-1 data, collected during the years 2011 and 2012 with a centre-of-mass energy of 7 and 8 TeV, respectively, corresponding to a total integrated luminosity of $3.1\,\text{fb}^{-1}$.

The LHCb experiment [2,3] is one of the four largest experiments located at the LHC. Although converted into a general-purpose forward detector, it was initially designed to study the decays of hadrons containing b or c quarks. For time-dependent studies, such as the ones presented in this document, the ability of properly identifying the initial flavour of the meson (known as *flavour tagging*) is fundamental. To this end, two flavour tagging algorithms are used: the opposite-side (OS) taggers and the same-side kaon (SSK) taggers, which exploit specific features of the incoherent production of $b\bar{b}$ quark pairs in pp collisions. Each tagging algorithm gives a tag decision and a mistag probability, the fraction of events with the wrong tag decision, $\eta \in [0, 0.5]$. The tag decision takes values $+1$, 1, or 0, if the signal meson is tagged as B_s^0, $\bar{B}_s^0$ or untagged, respectively. The fraction of events in the sample with a nonzero tagging decision gives the efficiency of the tagger, ε. The mistag probability is then calibrated to obtain the corrected per-event mistag probability, ω. This is used to determine the dilution factor, $\mathcal{D} = (1 - 2\omega)$, that rescales the efficiency of the tagger to quantify the fraction of the sample equivalent to perfectly tagged events. This effective efficiency is called tagging power, given by the product of the efficiency and the square dilution, $\varepsilon\mathcal{D}^2$.

2. – $B_s^0 \to J/\psi K^+K^-$

This decay proceeds predominantly by a tree-level $b \to c\bar{c}s$ transition, with a *CP*-violating phase (ϕ_s) that is very precisely predicted in the SM. Ignoring sub-leading (penguin) contributions, this phase can be related to the elements of the CKM quark-mixing matrix, V_{ij}, such that $\phi_s \approx -2\beta_s$, where $\beta_s = \arg\left[\frac{-V_{ts}V_{tb}^*}{V_{cs}V_{cb}^*}\right]$, leading to the expected value of $\phi_s^{SM} = -0.0364 \pm 0.0016$ rad [4]. The small uncertainty of this prediction, together with the great enhancement that can come from several NP models [5,6], makes this channel a golden mode. Apart from LHCb, it has also been measured by CDF [7], D0 [8], ATLAS [9] and CMS [10] .

The analysis performed by LHCb [11] entails the measurement of 9 main observables: a direct *CP*-violating parameter ($|\lambda|$), decay width and decay width difference between the two B_s^0 mass eigenstates, $B_{s(H)}^0$ and $B_{s(L)}^0$ (Γ_s, $\Delta\Gamma_s$), two polarization amplitudes ($|A_\perp|^2$, $|A_0|^2$), two strong-phases ($\delta_\parallel$, $\delta_\perp$), ϕ_s and the mass difference between the mass eigenstates, Δm_s. The direct *CP*-violating parameter is considered to be common to all polarization states (three polarizations of the ϕ and an S-wave) in the baseline fit. Checks with different λ_i, where i denotes the polarization state, were carried out, and found to be

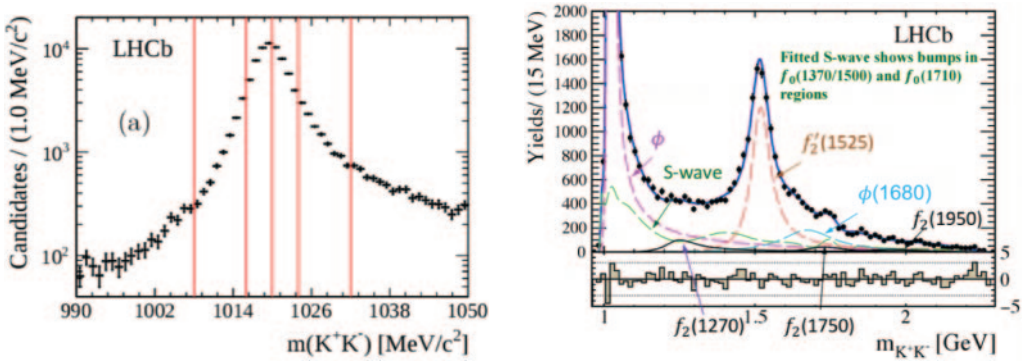

Fig. 1. – $m(K^+K^-)$ spectrum for the $B_s^0 \to J/\psi K^+K^-$ analysis, in the low (left) [11] and high (right) [12] mass region. The red lines in the left plot represent the binning, chosen such that it optimizes the statistics.

consistent with this assumption. The original analysis, performed with a mass window for the K^+K^- system around the $\phi(1020)$ resonance, $m(J/\psi K^+K^-) \in [5350, 5380]$ MeV/c^2, is dominated by the $B_s^0 \to J/\psi\phi$ mode and the S-wave fraction is rather small in comparison. Thus, only P-wave and S-wave contributions to the amplitudes are accounted for. No D-wave contribution is considered to enter the spectrum.

Detector effects such as angular and time acceptance, as well as the time resolution, are taken into account when performing the fit. The fitted data is background-subtracted, being the main peaking backgrounds the decays $B^0 \to J/\psi K^{*0}$ and $\Lambda_b^0 \to J/\psi p K^-$. The fit is performed separately for the 2 data-taking years, in 2 bins of trigger categories and 6 bins of the invariant mass of the K^+K^- system (shown in the left plot of fig. 1). The efficiencies related to the angular and time acceptances, as well as the time resolution, are modelled for each bin. The coupling between the P-wave and S-wave is computed using 6 $C_{\rm SP}$ factors [13] along the $m(K^+K^-)$ bins, with values contained in the $[0, 1]$ range. The effective tagging power for this analysis is $\varepsilon\mathcal{D}^2 = 3.73 \pm 0.15\%$. The obtained value for the CP-violating phase is $\phi_s = -0.058 \pm 0.049(\text{stat.}) \pm 0.006(\text{syst.})$ rad, being the angular acceptance the main source for the latter. This result is further combined with the one obtained in the $B_s^0 \to J\psi\pi^+\pi^-$ analysis [14], resulting in a measured value of $\phi_s = -0.010 \pm 0.039$ rad.

Another analysis has been peformed by LHCb for the high $m(K^+K^-)$ region [12], with a mass window $m(J/\psi K^+K^-) \in [5300, 5450]\,\text{MeV}/c^2$. In this region above the $\phi(1020)$ resonance, various waves (like a D-wave $f_2'(1525)$ resonance, not included in the previous measurement), contribute significantly to the decay, as can be seen in the right plot of fig. 1. The procedure is similar to the previous one, with some differences, such as the fact that the K^+K^- is modelled in this case. Also, some quantities, *e.g.*, the tagging power and the sWeights applied to get background-subtracted data [15], are computed separately for $m(K^+K^-) < 1050$ MeV and $m(K^+K^-) > 1050$ MeV. The main sources of background in this case are $\bar{B}^0 \to J/\psi K^-\pi^+$ and $\Lambda_b^0 \to J/\psi p K^-$. The resulting CP-violating phase is measured to be $\phi_s = -0.119 \pm 0.107(\text{stat.}) \pm 0.034(\text{syst.})$ rad. The dominant systematic source is the resonance modelling. This leads to a final ϕ_s combination (including the two $B_s^0 \to J\psi K^+K^-$ analysis done with Run-1 data) of $\phi_s = -0.025 \pm 0.045(\text{stat.}) \pm 0.008(\text{syst.})$ rad, dominating the world average (fig. 2).

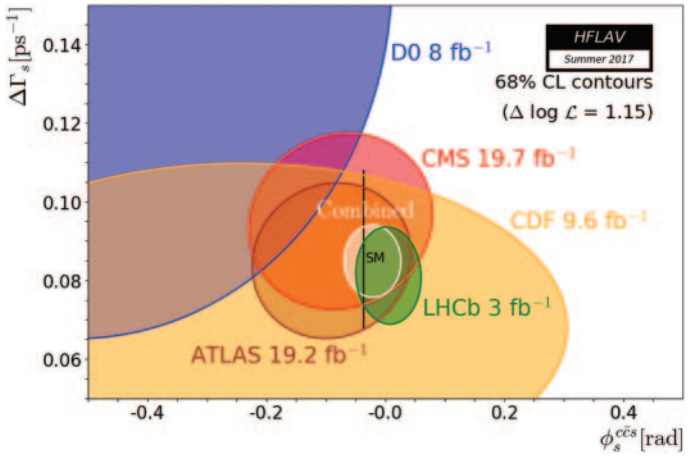

Fig. 2. – Individual 68% confidence level contours of ATLAS, CMS, CDF, D0 and LHCb in the $(\phi_s^{c\bar{c}s}, \Delta\Gamma_s)$, their combined contour (solid line and shaded area), as well as the SM predictions (thick black rectangle) as performed by HFLAV [16].

3. – $B_s^0 \to (K^+\pi^-)(K^-\pi^+)$

The $B_s^0 \to (K^+\pi^-)(K^-\pi^+)$ decay proceeds through a flavour-changing neutral current transition ($\bar{b} \to \bar{s}d\bar{d}$) dominated by a gluonic-penguin diagram in the SM. Its weak phase, $\phi_s^{d\bar{d}}$, is expected to be close to 0 in the SM [17]. New heavy particles could enter the loop that dominates the decay, therefore affecting the measurement. In order to improve the precision of this analysis with respect to previous studies [18], a two-dimensional mass window $m(K^\pm\pi^\mp) \in [750, 1600]$ MeV/c^2 is considered, with contributions from 9 decay channels, leading to a total of 19 polarization amplitudes. The differential decay rate for this channel contains an angular dependence, parametrized using spherical harmonics, and a mass dependence, which is described by barrier factors (using Blatt-Weisskopf functions), phase space factors and mass propagators. The latter are taken from a combination of scattering studies (phase) [19] and data (modulus) for spin-0 contributions, while for higher-spin components a relativistic Breit-Wigner is used.

The analysis procedure [20] is similar to the $B_s^0 \to J/\psi K^+K^-$ one. A first loose event selection is applied (including mass vetoes and cuts on particle identification variables), followed by a multivariate selection to suppress combinatorial background. Additional background sources, such as peaking backgrounds ($B^0 \to (K^+\pi^-)(K^-\pi^+)$, $B^0_{(s)} \to \phi(K^+\pi^-)$, $B^0 \to \rho(K^+\pi^-)$, Λ_b decays) and partially reconstructed decays are further subtracted applying sWeights in the $m(K^+\pi^-K^-\pi^+)$ spectrum. The detector effect in the acceptances is also taken into consideration, being the decay time acceptance parametrized by cubic splines. As for the decay time resolution, an analytical convolution is used with a Gaussian model, where both the width and the per-event decay time error are linearly related. The effective tagging power is found to be $\varepsilon\mathcal{D}^2 = 5.16 \pm 0.17\%$.

The large amount of polarization amplitudes entering the fit makes it of big complexity, thus largely benefitting from the usage of a new fitting framework based on GPUs [21] in order to properly determine the observables. The fit is then performed using two separate datasets for the 2 data-taking years, further split into 2 different trigger categories. With this, 19 polarization amplitudes are measured with the highest (for some of them

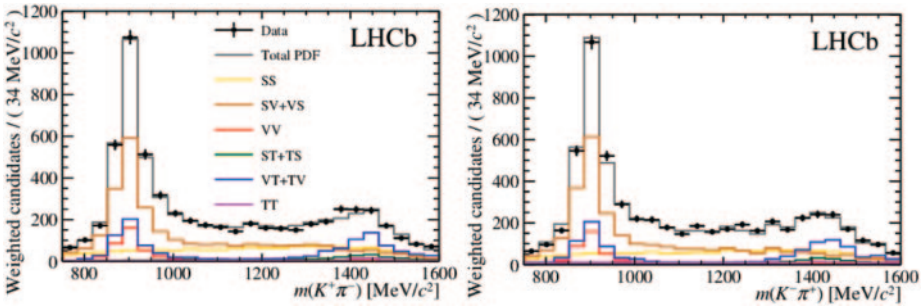

Fig. 3. – Fit projections on the $m(K^{\pm}\pi^{\mp})$ invariant mass [20].

first time) precision. The fit projections of the different contributions to the invariant mass of the $K^{\pm}\pi^{\mp}$ system are shown in fig. 3.

The longitudinal polarization is found to be relatively low, $f_L^{VV} = 0.208 \pm 0.032(\text{stat.}) \pm 0.046(\text{syst.})$, constituting and interesting input for penguin dynamics. Finally, the *CP*-violating phase is first measured for this channel, and found to be $\phi_s^{d\bar{d}} = -0.10 \pm 0.13(\text{stat.}) \pm 0.14(\text{syst.})$ rad, consistent with both the SM prediction and the result from the $B_s^0 \to \phi\phi$ measurement [22]. The main systematic source for this channel is related to the size of the simulation samples used for the multi-dimensional acceptances. Therefore, it is expected to experience a significant reduction in the future.

4. – $B_s^0 \to \phi\phi$

As for the previous cases, the $B_s^0 \to \phi\phi$ decay proceeds via a flavour-changing neutral current transition ($b \to ss\bar{s}$). As a penguin-dominated mode, its *CP*-violating phase is also expected to be close to 0 in the SM [23]. This decay was first observed and updated by the CDF Collaboration [24]. The analysis performed by the LHCb Collaboration [22] is twofold, consisting on a decay time-dependent measurement of $\phi^{ss\bar{s}}$, together with a time-integrated study in order to determine the triple product asymmetries for this decay.

Since the ϕ meson is close in mass to the $f_0(890)$ resonance, the amplitude of this channel takes into consideration both vector and scalar contributions, such that $A = A_{VV} + A_{VS} + A_{SS}$. An angular distribution is used to determine the *S*-wave fraction, while C_{SP} factors account for the interference between the *P*-wave, parametrized using a Breit-Wigner distribution, and the *S*-wave, described by a flat model. The *S*-wave fraction is very small, hence only the *P*-wave fraction is included in the simulation.

The analysis is very similar to the ones described before, for a ϕ mass window of $50\,\text{MeV}/c^2$ centred on the nominal ϕ mass, with a tagging power of $\varepsilon_{2011}\mathcal{D}^2 = 3.17 \pm 0.26\%$ and $\varepsilon_{2012}\mathcal{D}^2 = 3.04 \pm 0.24\%$. The studied sources of peaking backgrounds are $B^+ \to \phi K^+$, $B^0_{(s)} \to \phi\pi^+\pi^-$, found to have negligible contributions, and $\Lambda_b^0 \to \phi K^- p$, $B^0_{(s)} \to \phi K^*(892)^0$. The time acceptance in this case is data driven, using $B_s^0 \to D_s^+ (\to K^+K^-\pi^+)\pi^-$ as control mode, with an upper cut of 1 ps in the D_s^+ lifetime to align both samples as much as possible. The fit is done in 4 different trigger categories and 3 mass regions of the invariant masses of the kaon pairs (K^+K^-) to which each ϕ decays. Both the decay width and the decay width difference are taken from $B_s^0 \to J/\psi K^+K^-$, $B_s^0 \to J/\psi\pi^+\pi^-$ and implemented as Gaussian constraints. The fit projections for

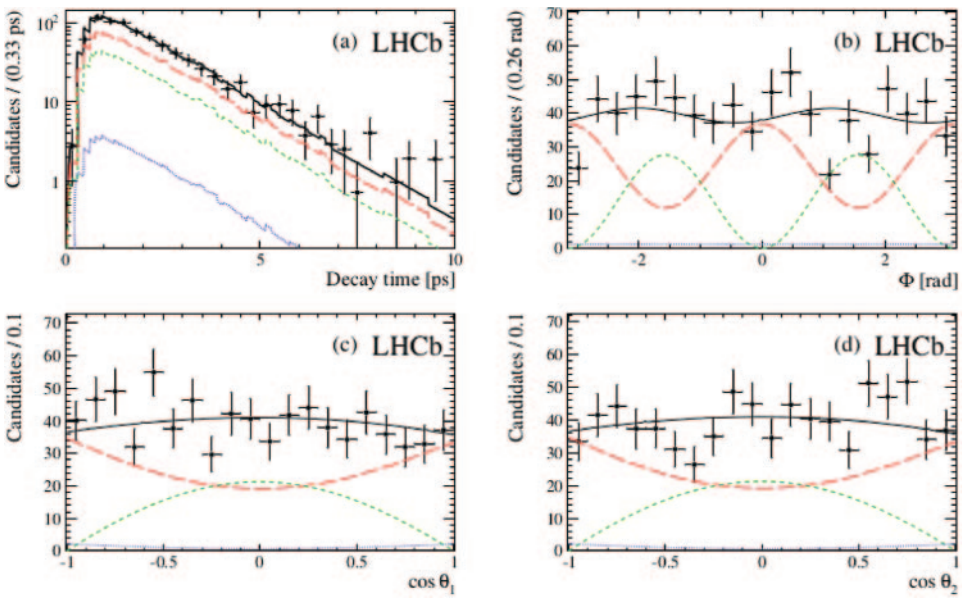

Fig. 4. – One-dimensional projections of the $B_s^0 \to \phi\phi$ fit for (a) decay time, (b) helicity angle Φ and the cosine of the helicity angles θ_1 (c) and θ_2 (d). The data are marked as points, while the solid lines represent the projections of the best fit. The CP-even P-wave, the CP-odd P-wave and S-wave components are shown by the long-dashed, short-dashed and dotted lines, respectively [22].

the different helicity angles are shown in fig. 4. The direct CP violation parameter, 3 polarization amplitudes and the strong phases are measured, apart from $\phi_s^{ss\bar{s}}$, which is found to be $\phi_s^{ss\bar{s}} = -0.17 \pm 0.15(\text{stat.}) \pm 0.03(\text{syst.})$ rad. The largest sources of systematic uncertainty are the decay time and angular acceptances. This result is consistent with the SM.

5. – Conclusions

In this document, the latest measurements from LHCb on the CP-violating phase ϕ_s^f using data from Run-1 have been reviewed. The world's best measurement for the $B_s^0 \to (K^+\pi^-)(K^-\pi^+)$ channel has been presented, $\phi_s^{ss\bar{s}} = -0.17 \pm 0.15(\text{stat.}) \pm 0.03(\text{syst.})$ rad, together with updated results on the $B_s^0 \to J/\psi K^+K^-$ (for the low and high mass regions) and $B_s^0 \to \phi\phi$ channels: $\phi_s^{d\bar{d}} = -0.10 \pm 0.13(\text{stat.}) \pm 0.14(\text{syst.})$ rad (dominating the world average) and $\phi_s^{c\bar{c}s} = -0.025 \pm 0.045(\text{stat.}) \pm 0.008(\text{syst.})$ rad, respectively.

While all the results presented are consistent with the SM predictions, room for NP still exists. The precision in the experimental measurements performed by LHCb is expected to significantly improve with the data from Run-2 data and the LHCb upgrade.

* * *

The author gratefully acknowledges the LHCb Collaboration and the financial support of ERC-StG-639068 and XuntaGal.

REFERENCES

[1] Kobayashi M. and Maskawa T., *Prog. Theor. Phys.*, **49** (1973) 652.
[2] LHCb Collaboration (Alves A. A. jr. *et al.*), *JINST*, **3** (2008) S08005.
[3] LHCb Collaboration (Aaij R. *et al.*), *Int. J. Mod. Phys. A*, **30** (2015) 1530022 (arXiv:1412.6352 [hep-ex]).
[4] Charles J. *et al.*, *Phys. Rev. D*, **84** (2011) 033005 (arXiv:1106.4041 [hep-ph]).
[5] Chiang C. W., Datta A., Duraisamy M., London D., Nagashima M. and Szynkman A., *JHEP*, **04** (2010) 031 (arXiv:0910.2929 [hep-ph]).
[6] Buras A. J., *PoS (EPS-HEP 2009)* (2009) 024 (arXiv:0910.1032 [hep-ph]).
[7] CDF Collaboration (Aaltonen T. *et al.*), *Phys. Rev. Lett.*, **109** (2012) 171802 (arXiv:1208.2967 [hep-ex]).
[8] D0 Collaboration (Abazov V. M. *et al.*), *Phys. Rev. D*, **85** (2012) 032006 (arXiv:1109.3166 [hep-ex]).
[9] ATLAS Collaboration (Aad G. *et al.*), *JHEP*, **08** (2016) 147 (arXiv:1601.03297 [hep-ex]).
[10] CMS Collaboration (Khachatryan V. *et al.*), *Phys. Lett. B*, **757** (2016) 97 (arXiv:1507.07527 [hep-ex]).
[11] LHCb Collaboration (Aaij R. *et al.*), *Phys. Rev. Lett.*, **114** (2015) 041801 (arXiv:1411.3104 [hep-ex]).
[12] LHCb Collaboration (Aaij R. *et al.*), *JHEP*, **08** (2017) 037 (arXiv:1704.08217 [hep-ex]).
[13] Xie Y., LHCb-INT-2012-017.
[14] LHCb Collaboration (Aaij R. *et al.*), *Phys. Lett. B*, **736** (2014) 186 (arXiv:1405.4140 [hep-ex]).
[15] Pivk M. and Le Diberder F. R., *Nucl. Instrum. Methods A*, **555** (2005) 356 (physics/0402083 [physics.data-an]).
[16] HFLAV Collaboration (Amhis Y. *et al.*), *Eur. Phys. J. C*, **77** (2017) 895 (arXiv:1612.07233 [hep-ex]).
[17] Descotes-Genon S., Matias J. and Virto J., *Phys. Rev. D*, **76** (2007) 074005; **84** (2011) 039901 (arXiv:0705.0477 [hep-ph]).
[18] LHCb Collaboration (Aaij R. *et al.*), *JHEP*, **07** (2015) 166 (arXiv:1503.05362 [hep-ex]).
[19] Pelaez J. R. and Rodas A., *Phys. Rev. D*, **93** (2016) 074025 (arXiv:1602.08404 [hep-ph]).
[20] LHCb Collaboration (Aaij R. *et al.*), *JHEP*, **03** (2018) 140 (arXiv:1712.08683 [hep-ex]).
[21] Santos D. M., Cartelle P. A., Borsato M., Chobanova V. G., Pardinas J. G., Martinez M. L. and Ramos Pernas M., arXiv:1706.01420 [hep-ex].
[22] LHCb Collaboration (Aaij R. *et al.*), *JHEP*, **10** (2015) 053 (arXiv:1508.00788 [hep-ex]).
[23] Charles J. *et al.*, *Phys. Rev. D*, **84** (2011) 033005 (arXiv:1106.4041 [hep-ph]).
[24] CDF Collaboration (Acosta D. *et al.*), *Phys. Rev. Lett.*, **95** (2005) 031801 (hep-ex/0502044).